

# We are IntechOpen, the world's leading publisher of Open Access books Built by scientists, for scientists

6,900

Open access books available

185,000

International authors and editors

200M

Downloads

Our authors are among the

154

Countries delivered to

TOP 1%

most cited scientists

12.2%

Contributors from top 500 universities



WEB OF SCIENCE™

Selection of our books indexed in the Book Citation Index  
in Web of Science™ Core Collection (BKCI)

Interested in publishing with us?  
Contact [book.department@intechopen.com](mailto:book.department@intechopen.com)

Numbers displayed above are based on latest data collected.  
For more information visit [www.intechopen.com](http://www.intechopen.com)



# Application of Infrared Spectroscopy in Catalysis: Impacts on Catalysts' Selectivity

*Patricia Concepción*

## Abstract

Catalysis plays an important role in sustainable chemistry, enabling the development of more efficient processes by minimizing the consumption of energy and reducing the generation of by-products. The design of efficient catalysts is a key point in this respect, where spectroscopy confers fundamental knowledge at the molecular scale. Among the different spectroscopies, infrared (IR) spectroscopy is of great interest, enabling information about the nature of active species and the reaction mechanism, leading to precise structure-activity correlations, which are a key point in the design of new catalysts. Moreover, the dynamic behavior of the catalysts under working conditions can be also monitored by IR spectroscopy, where structural modifications of working catalysts have strong repercussion in catalysis. In this chapter, interesting examples will be discussed, related to industrial relevant processes, like Fischer-Tropsch synthesis, ethylene oligomerization, synthesis of aniline from nitrocompounds, and the dehydration of aldoximes to nitriles.

**Keywords:** catalysis, Fischer-Tropsch, ethylene, nitrobenzene, aldoximes, CO

## 1. Introduction

One of the greatest challenges in the current chemical industry is the development of high-efficient processes with increased selectivity and reduced generation of by-products. This has motivated extensive research in the last years focused on the use of alternative renewable feedstocks and on the development of less energetic reaction pathways or radically new chemical processes [1]. Catalysis plays an important role in defining new eco-efficient processes, where improvements in catalyst design and in catalytic reactor engineering are key elements that have to be linked to each other. The rational development of catalysts with enhanced catalytic performance relays on a fundamental knowledge of the catalytic process encompassing the reaction mechanism, rate-limiting reaction step, and the nature of active sites of the catalyst, where spectroscopy and theoretical studies are key aspects [2, 3]. Among the different types of spectroscopies, infrared (IR) spectroscopy is one of the most powerful techniques for the characterization of catalytic systems. This is easily demonstrated by the high number of studies found in the literature focused on the characterization of catalysts involved in industrial relevant processes [4–8]. In recent years, thanks to the technological advances allowing enhanced spectral (signal/noise level), temporal (rapid scan and step scan), and

spatial (IR microscopy) resolution, with cutting-edge values in the  $\mu\text{s}$  and  $\mu\text{m}$  range, respectively, and by the development of new catalytic IR cells enabling transient studies in the  $\mu\text{s}$  range [9], a lot of interest has emerged in studying the catalyst under conditions resembling those encountered in catalysis, i.e., under “in situ” or “operando” conditions [10, 11]. In addition, extensive effort is being placed in coupling IR spectroscopy to other spectroscopies (UV–Vis, EXAFS, AP-XPS) [12, 13], expanding the information obtained for a given catalytic system. In the present chapter, the application of IR spectroscopy in catalysis is described providing interesting examples to illustrate how IR spectroscopy allows accurate characterization of catalyst surface sites and the identification of active sites in working catalysts enabling to establish structure-activity correlations, being this key point in the design of new catalysts. Moreover, the analysis of the reaction mechanism and rate-determining reaction steps by means of time- and temperature-resolved IR spectroscopy will also be discussed. Some examples related to relevant industrial processes like Fischer-Tropsch synthesis, ethylene oligomerization, dehydration of aldoxime compounds to their corresponding nitriles, and hydrogenation of nitrobenzene to aniline or azobenzene will be provided in order to illustrate the great potential of IR spectroscopy in the field of catalysis.

## **2. IR spectroscopy in catalyst characterization**

IR spectroscopy provides detailed molecular information of the nature of adsorbed species on a catalyst surface, their interaction strength, and evolution under controlled atmospheres and temperatures. Using specific probe molecules, it allows to extract relevant information of the nature of surface sites on a catalyst, such as acid, base, and redox sites, surface defects, and the dynamic behavior of those sites under reaction conditions. Moreover, thermodynamic data such as entropy and enthalpy of molecular adsorption on a specific surface site [14, 15] and kinetic data can be accurately obtained. Altogether and comparing the IR data with macro-kinetic catalytic data, it assists in defining precise structure-activity correlations on a working catalyst, which is crucial in new catalyst designs. On the other hand, IR spectroscopy can be applied under a diverse set of environments: in air, in vacuum or in the presence of reactants under controlled low pressure, at cryogenic or high temperatures, and under more relevant catalytic conditions, including gases at atmospheric or even at higher pressures (20–30 bar) and liquids, allowing catalyst research to be performed under a wide range of reaction conditions. In the following sections, the application of IR spectroscopy in catalysis, especially in unraveling the nature of surface sites, discerning those who acts as active sites, and determining the reaction mechanism and rate-limiting step, will be discussed through selected illustrative examples.

### **2.1 Determination of the nature of surface sites**

The surface of industrial catalysts is quite complex, comprising sites of different natures such as Brønsted ( $\text{H}^+$ ) acid sites, Lewis acid and base sites, transition metals with redox properties, and surface defects. Due to this huge number of sites, it is sometimes hard to get information about the intrinsic properties of the surface sites present in a working catalyst and, more importantly, to identify those who are involved in the catalytic process, called active sites. In this direction, IR spectroscopy with the aid of probe molecules has been proven as a very powerful characterization technique. Such probe molecules interact with specific surface sites resulting in a shift of their characteristic vibrational mode providing information

about the chemical properties of the surface site (i.e., oxidation state, coordination, and chemical environment) and in the case that the adsorption coefficient of the corresponding IR mode is known, allowing their quantification. Many probe molecules are reported in the literature enabling information of specific aspects of the catalyst surface [16–18]. The choice of an appropriate molecule is a crucial point in the surface characterization, and often the combined use of several molecules is required for a comprehensive knowledge of the catalyst surface sites. Perhaps, the most widely known application of probe molecules in IR spectroscopy is related to the identification and quantification of acid sites (Lewis and Brønsted) in a catalyst [19, 20]. Several base molecules have been used for that purpose, where weak bases like  $H_2$ ,  $N_2$ ,  $CO$ , and  $NO$  have been proven as very sensitive to the local environment and oxidation state of the surface site [21, 22], while strong bases, like pyridine and ammonia, are less sensitive but very specific to the presence of Brønsted acid sites [23, 24]. The use of other probe molecules, like acetonitrile, alcohols, and thiols, has also been reported [25]. In this direction, an interesting example with important industrial repercussion is the search of efficient catalysts for the elimination of  $NO_x$  emissions, where the selective catalytic reduction (SCR) of  $NO_x$  with ammonia ( $NH_3$ -SCR) or hydrocarbons (HC-SCR) is today one of the most efficient technologies. In this context, Cu-exchanged zeolites have shown interesting catalytic performance, where the identification of the nature of copper species is clue but highly challenging due to the coexistence of many different species such as isolated  $Cu^{2+}$ ,  $Cu^+$ ,  $Cu(OH)^+$ , dimeric  $[Cu-O-Cu]$ , sub-nanometric  $Cu_xO_y$  clusters, and/or  $CuO$  and  $Cu_2O$  aggregates [26–28]. Despite the massive number of investigations on these systems, there is still controversy about the nature of active sites, mainly due to the wide range of catalysts explored in the literature containing a mixture of multiple copper sites. Therefore, one way to overcome the complexity of many industrial catalysts is to try to design catalysts containing well-defined uniform sites and use them as model systems in both catalytic and spectroscopic studies. Following this hint, Cu-exchanged zeolites with uniform isolated sites (Cu-SAPO-34 and Cu-SSZ-13) have been prepared in our group by a hydrothermal synthetic approach [29–31]. Both catalysts show high activity and stability in the  $NH_3$ -SCR reaction, making them interesting candidates for the investigation of active sites in the SCR reaction. IR spectroscopy of  $CO$  and  $NO$  adsorption as probe molecules, combined with theoretical modeling of the vibrational frequencies, has allowed precise identification of  $Cu^{2+}/Cu^+$  species located either in the 8-ring or 6-ring of the zeolite structure, as well as the identification of  $Cu-O-Cu$  dimeric species, resolving some of the controversy in the assignation of IR band frequencies present in the literature and establishing the role of isolated  $Cu^{2+}/Cu^+$  ions as active sites in the  $NH_3$ -SCR [32].

Among the different types of industrial catalysts, metal-based catalysts containing noble metals like Pt, Pd, and Rh and non-noble metals like Ni, Co, and Ru are used in many industrial processes. The catalytic activity and selectivity of this class of catalysts are strongly influenced by their particle size and morphology, electronic state of surface metal atoms, and metal interfaces or heterojunctions in the metal particle, where a comprehensive knowledge of these parameters is essential in understanding their catalytic performance. To achieve that, the combination of several spectroscopic tools is strongly required, being IR of  $CO$  as probe molecule of great interest. Based on the shift of the  $\nu(C\equiv O)$  frequency, metal particles exhibiting different facets like the (111) (100) (110) crystallographic planes, as well as the presence of undercoordinated metal atoms located in steps and corners of the metal particle, can be easily detected [33, 34]. For example, by combining IR of  $CO$  as probe molecule with theoretical vibrational simulations obtained by the density functional theory (DFT) method, gold atoms of different natures have been



investigated in supported gold nanoparticle catalysts. Specifically, gold atoms with different coordination degrees (for instance, in the edge and corners of the particle), electron density (for instance,  $\text{Au}^{\delta+}$  atoms located in the perimeter of the gold particle in close contact with the support), and oxidation state ( $\text{Au}^{3+}$ ,  $\text{Au}^+$  and  $\text{Au}^0$ ) have been accurately defined [35].

Finally, the characterization of surface base sites in a catalyst using IR spectroscopy of probe molecules (like  $\text{CO}_2$ , trichloromethane, acetylene, and pyrrole) is less studied, mainly due to the complexity of some of the probe molecules when adsorbed on the catalyst surface [17, 36]. For example,  $\text{CO}_2$  adsorption on basic surface sites leads to several types of carbonate species which hinder accurate identification of surface base properties [37].

## 2.2 Determination of the nature of active sites: structure-activity correlation

The main challenge in spectroscopy, and specifically in IR spectroscopy, is to differentiate the catalytic active sites which are directly involved in the reaction mechanism, from the rest of sites normally present on the surface of working catalysts. Only in this case, it is possible to define accurate structure-activity correlations, which allows to direct the synthesis of new catalysts. Identification of active sites is not always straightforward and requires a multidisciplinary approach, combining surface characterization with catalytic data and, if possible, with theoretical calculations. In the following subsections, we will provide some examples of our work where active sites have been accurately identified.

### 2.2.1 Nature of active sites in the dehydration of aldoximes to nitriles on heterogeneous ceria catalysts

Nitriles are precursors for a wide range of organic products like carboxylic acids, amines, ketones, and amides. The most efficient route for the synthesis of nitriles is the dehydration of aldoximes that can easily be obtained from the corresponding aldehydes. Homogeneous catalytic systems such as  $\text{Pd(II)}$  complexes with a phosphino-oxime ligand [38],  $\text{Co(II)Cl}_2$  [39],  $\text{Ga(OTf)}_3$  [40], and  $\text{Fe(ClO}_4)_3$  [41] are employed with interesting performance but presenting important limitations such as catalyst recovery, use of hazardous organic solvents, and long reaction time. Therefore, a lot of attention is paid in developing alternative heterogeneous catalysts. Among the different heterogeneous catalysts reported in the literature [42, 43], nanocrystalline ceria ( $\text{nCeO}_2$ ) stands as a very promising catalyst in the dehydration of a variety of aldoximes (including alkyl and cycloalkyl aldoximes) to the corresponding nitriles at moderate temperature ( $149^\circ\text{C}$ ) with yields around 80–97% [44]. The catalyst shows good stability and recyclability after several uses. While both acid and basic sites are discussed in the literature for aldoxime dehydration, there is no clear understanding about the role of each of them in the reaction mechanism. In order to shed light into the participation of acid and base sites in the reaction mechanism, we performed a detailed IR study on  $\text{nCeO}_2$  compared with other catalysts ( $\text{CeO}_2$ ,  $\text{MgO}$ ,  $\text{Al}_2\text{O}_3$ , and  $\text{TiO}_2$ ). The different catalysts are studied in the dehydration of 4-methoxybenzaldehyde oxime, where the initial reaction rate follows the order  $\text{nCeO}_2 > \text{MgO} > \text{Al}_2\text{O}_3 > \text{CeO}_2 > \text{TiO}_2$ . Surface characterization is done using CO and  $\text{CHCl}_3$  as probe molecules. Based on the IR spectra of CO adsorption (**Figure 1A**), the acid strength of the different catalysts (being proportional to the red  $\nu(\text{C}\equiv\text{O})$  shift) can be ranked in the order  $\text{Al}_2\text{O}_3 > \text{TiO}_2 > \text{MgO} > \text{nCeO}_2 > \text{CeO}_2$ , while the number of surface acid sites (peak area normalized by the catalyst surface area), called surface acid density, follows a different order  $\text{CeO}_2 > \text{TiO}_2 > \text{nCeO}_2 > \text{Al}_2\text{O}_3 > \text{MgO}$ . In the same way, based on the

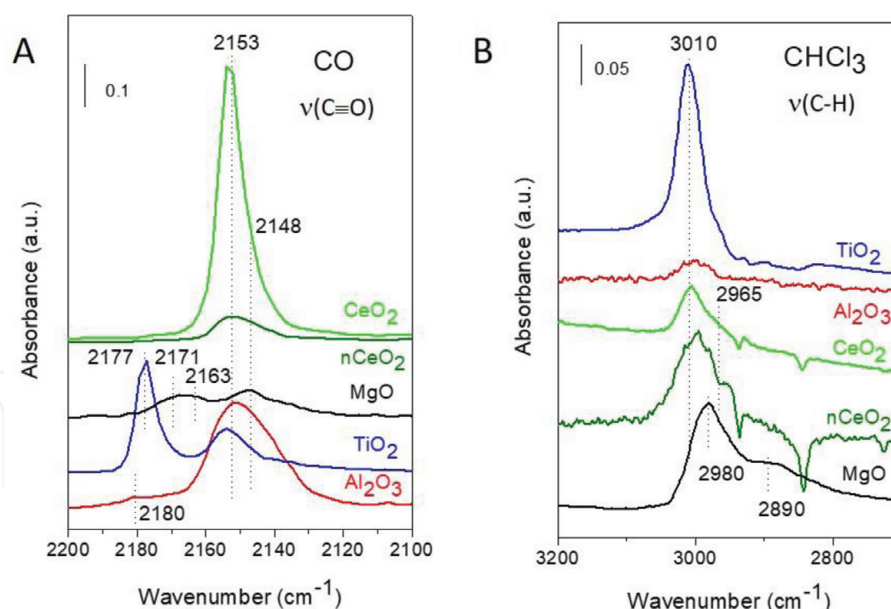
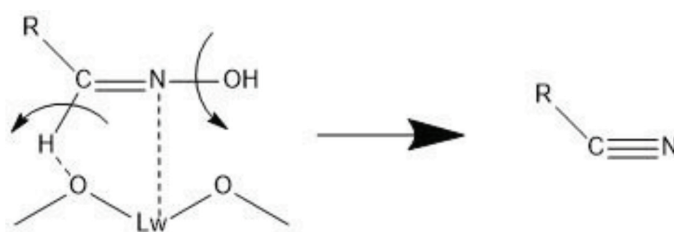


**Figure 1.**  
 (A) IR spectra of CO adsorption at saturation coverage on the different catalysts. (B) IR spectra of  $\text{CHCl}_3$  adsorption at saturation coverage on the same catalysts. All spectra are normalized to sample weight.

IR spectra of  $\text{CHCl}_3$  adsorption (**Figure 1B**), the basic strength (being proportional to the blue  $\nu(\text{C-H})$  shift) can be ranked in the order  $\text{MgO} > \text{nCeO}_2 > \text{CeO}_2 > \text{TiO}_2 > \text{Al}_2\text{O}_3$ . The same order can be applied for the surface base density.

Once the catalyst acid and base sites are established, the “in situ” dehydration of propionaldehyde oxime is studied by IR spectroscopy in order to understand how the presence of those sites influences the reactivity of the samples. The observed IR red shift of both  $\nu\text{C=N}$  (from  $1640\text{ cm}^{-1}$  in the gas phase to  $1646\text{ cm}^{-1}$  on  $\text{nCeO}_2$  and  $1667\text{ cm}^{-1}$  on  $\text{Al}_2\text{O}_3$ ) and  $\nu\text{N-OH}$  vibrations ( $1028\text{ cm}^{-1}$  in the gas phase to  $1037\text{ cm}^{-1}$  on  $\text{nCeO}_2$  and  $1051\text{ cm}^{-1}$  on  $\text{Al}_2\text{O}_3$ ), suggests a mechanism for which the activation of propionaldehyde oxime involves an N-bond complex to a surface Lewis acid site increasing in that way the  $\text{C=N}$  and  $\text{N-OH}$  bond strength [45], followed by  $\text{N-OH}$  bond elimination and  $\text{C-H}$  cleavage with subsequent water and nitrile formation (**Scheme 1**). This differs to the conventional oxidative dehydration mechanism (i.e., interaction of the oxygen of the oxime with Lewis acid sites) for which a blue shift of both vibrations would be expected [45].

In addition, notice that in general the shift in the IR vibration of an adsorbed molecule reflects the degree of bond activation which is proportional to their catalytic reactivity. However, such a correlation is not found in this case, where the observed shift of the  $\text{N-OH}$  vibration is proportional to the sample acid strength, but doesn't match to the catalyst activity. Thus, Lewis acid sites, while being involved in the reaction mechanism, seems not to be a determinant factor for the catalytic activity. On the contrary, considering that both  $\text{nCeO}_2$  and  $\text{MgO}$  samples, with the highest basic strength, are the most active catalysts, surface basicity should



**Scheme 1.**  
 Proposed mechanism for the dehydrogenation of aldoximes to nitriles on metal oxide heterogeneous catalysts.

play a decisive role in the reaction mechanism. Basic sites are involved in the C-H bond cleavage, which from the IR and catalytic studies can be proposed as the rate-limiting step of the reaction. In conclusion, both Lewis acid sites and basic sites are involved in the reaction mechanism, being Lewis acid sites involved in the adsorption of the oxime, while strong basic sites are required for C-H activation.

In this way, combining IR data with catalytic data, the highest catalytic activity of the nCeO<sub>2</sub> can be ascribed to an appropriate number of surface acid sites enabling the activation of the oxime and strong basic sites favoring C-H cleavage. While similar strong basic sites are present on MgO, the lower surface density of acid sites explains its lower activity than nCeO<sub>2</sub>. Moreover, owing to the basic character of both nCeO<sub>2</sub> and MgO, desorption of the nitrile from the catalyst surface is favored avoiding secondary reactions and enhancing catalyst stability.

### 2.2.2 Nature of active sites in ethylene oligomerization reaction

Ethylene oligomerization is an interesting chemical route of industrial importance for the production of linear and branched higher olefins. Those olefins, depending on their carbon number, show several applications, for example, comonomers in polyethylene industry (C<sub>4</sub>–C<sub>6</sub>), as plasticizer alcohols (C<sub>8</sub>–C<sub>10</sub>), as synthetic lubricants (C<sub>10</sub>–C<sub>12</sub>), in the detergent industry (C<sub>12</sub>–C<sub>16</sub>), and as lube oil components or in surfactant manufacture (C<sub>16</sub>–C<sub>18</sub>). Industrially, the process takes place in liquid phase using homogeneous transition metal complexes as catalysts and alkyl aluminum compounds as activators [46]. Owing to the limitations of the actual industrial process, such as difficulty to separate the catalyst from oligomers, increase of operational cost, and broad carbon number distribution of products, the search of alternative heterogeneous solid catalysts is very interesting from both economic and environmental points of view. In this sense, nickel loaded on acidic aluminosilicates such as zeolites and amorphous mesoporous supports has attracted great attention as efficient and environmentally friendly heterogeneous catalysts for ethylene oligomerization, although they suffered from catalyst deactivation with time of stream (TOS) [47]. Recently, our group developed a bifunctional catalyst comprised of Ni loaded on nanocrystalline zeolite HBeta (Ni-HBeta) with high catalytic activity and stability during the oligomerization process [48]. Ethylene conversions of ~90% at 2.5 wt% Ni loading in the Ni-HBeta catalyst under conventional reaction conditions (T = 120°C, P<sub>tot</sub> = 35 bar, P<sub>C<sub>2</sub>H<sub>4</sub></sub> = 26 bar, WHSV = 2.1 h<sup>-1</sup>) are obtained without apparent signs of deactivation within 1–9 h TOS. Despite the high promising features displayed by Ni-based catalysts, the nature of active sites (isolated Ni<sup>+</sup> and/or Ni<sup>2+</sup>) remained under debate, being subject of intense research studies in the last years [49–52]. To this aim, catalytic studies with high temporal resolution in the earliest stage of the reaction monitored by a combined gas chromatograph (GC) and mass spectrometry (MS) analysis technique and coupled with “in situ” IR-CO surface titration spectroscopic studies are performed in our group in order to identify the nature of the active Ni sites for ethylene oligomerization in the Ni-HBeta catalyst [53]. Catalysts with different nickel loadings (1, 2.5, 5, and 10 wt%) are studied. Specification of the nature of nickel sites monitored by IR of CO as probe molecule shows in all samples isolated Ni<sup>2+</sup> cations in ion exchange positions of the zeolite and isolated Ni<sup>2+</sup> interacting with silanol groups of internal defects (hydroxyl nests) or stacking faults of the nanocrystalline beta zeolite. Indeed, the IR-CO spectra of the activated 5wt%Ni-HBeta catalyst show IR bands at 2214 and 2207 cm<sup>-1</sup> assigned to carbonyls of isolated Ni<sup>2+</sup> ion exchange cations [51, 54] and an IR band at 2196 cm<sup>-1</sup> attributed to isolated Ni<sup>2+</sup> interacting with silanol groups [55], in addition to IR bands at 2175, 2164, 2156, and 2143, 2131 cm<sup>-1</sup>



attributed to CO interacting with Brønsted acid sites, aluminols, silanols, and physically adsorbed CO, respectively (**Figure 2**).

Interestingly, independent of the nickel loading in the Ni-HBeta sample, the time-resolved GC-MS catalytic studies performed in a low-dead-volume catalytic setup, working at 1 bar, 120°C, and WHSV of 33 h<sup>-1</sup> (**Figure 3A**), show a significant loss of ethylene conversion in parallel to a decrease in the butene concentration at the very early reaction stage (first 10 min) before achieving pseudo-steady-state activity at TOS of 30 min. The short time frame where the initial loss of activity occurs prevents their detection in a conventional high-pressure reactor setup, where all catalysts are shown to remain stable up to 9 h TOS. Coupled to the catalytic studies, IR studies at the same experimental conditions are performed using a low-volume IR catalytic cell. The “in situ” IR ethylene oligomerization reaction is stopped at different stages of the reaction (10 s, 8 min, 30 min, and 70 min) and the nature of Ni sites titrated by IR of CO as probe molecule. Since all catalysts displayed similar trends, the 5wt%Ni-HBeta catalyst is taken as representative in the following discussion. After “in situ” reaction with ethylene in the IR catalytic cell, a sharp reduction in the intensity of the IR bands related to the isolated Ni<sup>2+</sup> ions is noticed even after only 10s of reaction (**Figure 3B**). The decrease in intensity is particularly significant for the higher frequency bands at 2214 and 2207 cm<sup>-1</sup> related to the ion exchanged Ni<sup>2+</sup> ions with stronger Lewis acid character, while that at 2196 cm<sup>-1</sup> of less acidic isolated Ni<sup>2+</sup> interacting with silanol groups is much less affected; meanwhile, Brønsted acid sites at 2175 cm<sup>-1</sup> are also considerably reduced in intensity. In addition, dicarbonyl Ni<sup>+</sup> bands at 2138 and 2095 cm<sup>-1</sup> [56] are clearly detected at low CO coverage since the very early reaction stage, increasing in intensity during the course of the reaction (spectra not shown).

Linking the IR and GC-MS data (**Figure 3C**), Ni<sup>+</sup> ions cannot be considered as active site since the intensity of the IR bands of Ni<sup>+</sup> ions increases with reaction time, while the catalytic activity decreases. Despite this, a clear parallelism between

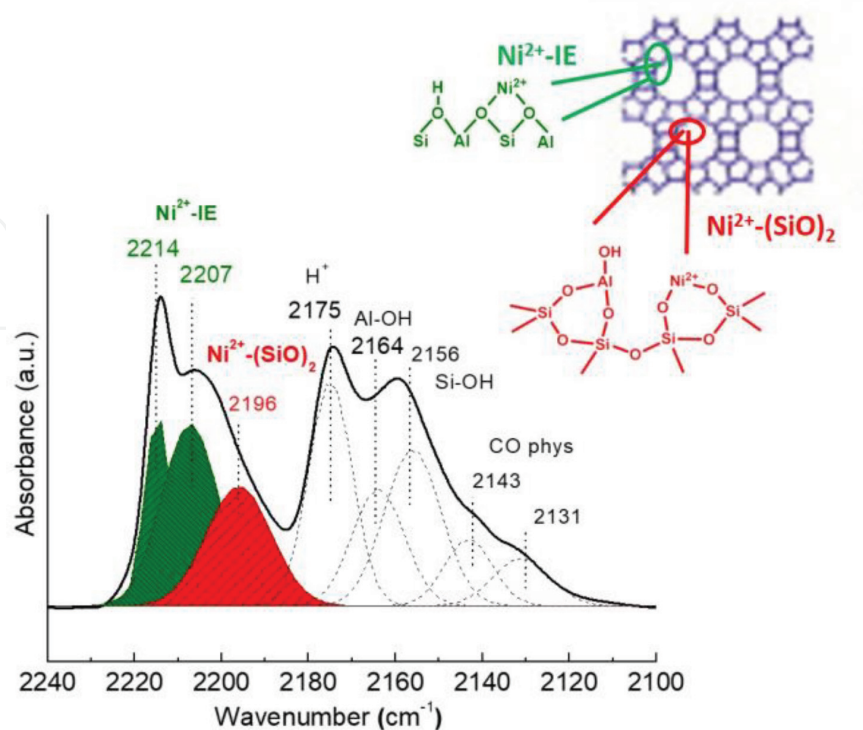


**Figure 2.**  
 IR spectra of CO adsorption at saturation coverage and at -175°C on the 5wt%Ni-HBeta sample activated in N<sub>2</sub> flow (20 ml/min) at 300°C for 3 h.



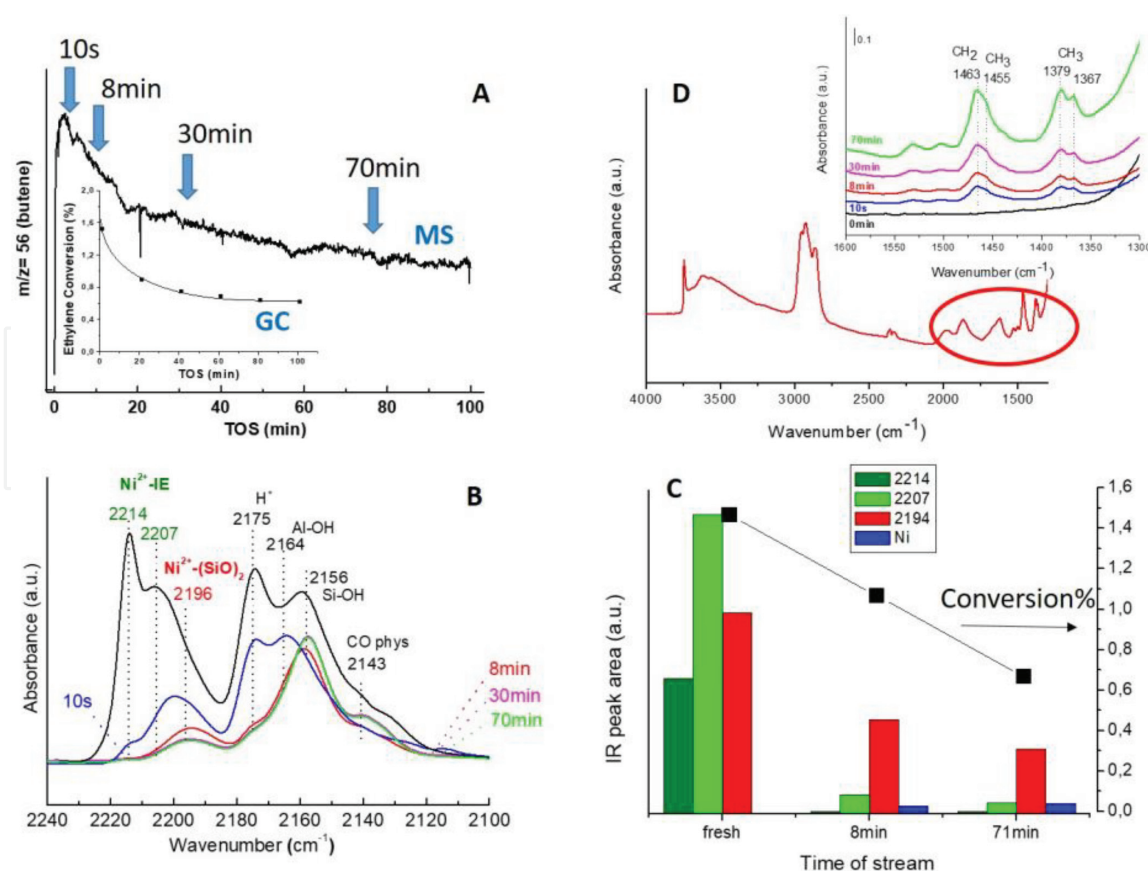


**Figure 3.**

(A) Time-resolved GC–MS analysis in the ethylene oligomerization reaction performed at 1 bar and 120°C on the 5wt%Ni-HBeta sample. The arrows correspond to the reaction stages where surface titration by IR–CO is performed. (B) IR spectra of CO adsorption at –175°C and at saturation coverage on the 5wt%Ni-HBeta sample stopped at selected reaction times. (C) Evolution in the concentration of the different nickel sites in the working 5wt%Ni-HBeta sample and their correlation with catalytic data (conversion). (D) The “in situ” IR spectra under ethylene oligomerization reaction at 1 bar and 120°C and at different TOS highlighting hydrocarbon formation.

the reduction in intensity of the IR bands of isolated  $\text{Ni}^{2+}$  ions and the initial decline in ethylene conversion rate is observed, implying that the two phenomena should be closely related. Significantly, while isolated ion exchange  $\text{Ni}^{2+}$  ions (IR bands at 2214 and 2207  $\text{cm}^{-1}$ ) become almost totally blocked in the first seconds of the reaction,  $\text{Ni}^{2+}$  ions interacting with silanol groups (IR band at 2196  $\text{cm}^{-1}$ ) remain accessible under reaction conditions and can accordingly be considered as the true catalytic active sites under steady-state conditions. The blocking of the most acid  $\text{Ni}^{2+}$  and Brønsted acid sites under reaction conditions is due to irreversibly adsorbed hydrocarbons formed from the very early stages of reaction as detected in the “in situ” IR spectra (**Figure 3D**). In conclusion, these results highlight the importance of nickel sites of intermediate Lewis acid strength in order to design efficient ethylene oligomerization catalysts.

### 2.2.3 Nature of active sites in the Fischer-Tropsch reaction

The Fischer-Tropsch (FT) reaction has gained renewed interest in the last years as an alternative route to produce high-quality liquid fuels from alternative sources to petroleum, such as natural gas, coal, and biomass [57]. In the FT process, cobalt-based catalysts have preferentially been employed due to their high stability, low activity for the competitive reverse water gas shift reaction (WGSR), and high selectivity to long-chain n-paraffins compared to alternative catalysts based on

iron [58]. Due to the interest in this process, a lot of research has been devoted to prepare novel catalysts with improved catalytic behavior. One conventional way to improve the catalytic activity is increasing the metal dispersion (i.e., decreasing particle size), but unexpectedly a low reaction rate and a low selectivity to the desired long-chain hydrocarbons have been observed in the FT process when decreasing the cobalt particle size below 8–9 nm [59, 60]. This trend differs from the classical structure sensitivity behavior, and the reason behind has been a long-lasting debate in the literature. Particularly, the presence of unreduced Co species due to the lower reducibility of small Co nanoparticles and the reoxidation of Co sites under reaction conditions in highly dispersed catalysts [60–64] have been the most widely discussed issues. In order to understand this nonclassical particle size-dependent activity, cobalt nanoparticles with a homogenous particle size distribution from 5.6 to 10.4 nm are prepared in our laboratory using a reverse micellar synthesis procedure and deposited onto a surface-silylated ITQ-2 delaminated pure silica zeolite [65]. As reference, a Co/SiO<sub>2</sub> catalyst with Co particle size of 141 nm is also studied. The metal loading in all samples is 10 wt%. The high reducibility of the catalysts and their homogeneous particle size distribution make them ideal candidates as model systems for investigating the aforementioned catalytic behavior. Spectroscopic studies combined with catalytic studies under FT conditions (P = 20 bar and T = 220°C) are performed. In the catalytic studies, the intrinsic catalytic activity (TOF) decrease with decreasing Co particle size from 10.4 to 5.6 nm remains constant for particle sizes above 10.4 nm, according to the literature. The evolution of the cobalt sites under FT reaction conditions is nicely followed in the “in situ” IR studies performed at ambient pressure under syngas flow and at increasing temperatures (25–220°C) (**Figure 4**). All samples show similar trend, where at 25°C two IR bands at 2048 cm<sup>-1</sup> associated with linearly CO adsorbed on fcc Co<sup>0</sup> sites [66] and at 1625 cm<sup>-1</sup> due to adsorbed water are observed. Increasing the temperature to 150 and 200°C, there are no bands observed in the Co-carbonyl region, probably due to a complete blockage of the surface sites and due to CO dissociation and the growth of adsorbed H<sub>x</sub>C intermediate species. Indeed, a band at 612 cm<sup>-1</sup> is observed in the low-frequency range, associated with adsorbed oxygen atoms (i.e., Co-O) [67]. Finally, increasing the temperature to

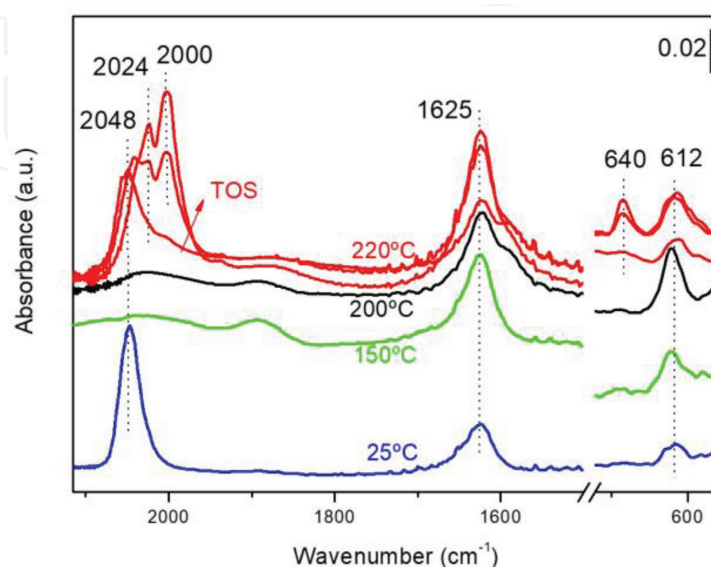


**Figure 4.**  
 FTIR spectra of the Co/ITQ-2 sample with 10.4 nm Co particle size under FT reaction conditions at 1 bar and at 25, 150, 200, and 220°C. Each spectrum is recorded after 45 min at each temperature. At 220°C the IR spectra are recorded at 120, 210, and 240 min time on stream (TOS).

220°C, Co-carbonyls are rapidly restored, due to desorption of reaction intermediate species leaving free cobalt metal sites for CO adsorption. Concomitantly, a progressive shift in the Co-carbonyl IR band is observed from 2048  $\text{cm}^{-1}$  to 2024 and 2000  $\text{cm}^{-1}$  with increasing reaction time at 220°C, where the 2024 and 2000  $\text{cm}^{-1}$  IR bands are related to unsaturated or low coordinated cobalt surface sites located in defect sites or on more open crystallographic cobalt planes [68, 69]. Being this shift in the IR bands irreversible, it is ascribed to cobalt surface reconstruction from an fcc structure to a more open crystallographic structure, the last one behaving as the true active site under working conditions [65]. Notice the parallel appearance of an IR band at 642  $\text{cm}^{-1}$  ascribed to cobalt-carbon species [70, 71] which provides the first experimental evidence for the role of carbon atoms in promoting surface reconstruction of the cobalt particle under FT conditions, in agreement to previous DFT calculations [72].

Notoriously, on the sample with the smallest Co particle size (5.6 nm) and lower catalytic activity (**Figure 5A**), a band at 2060  $\text{cm}^{-1}$ , not observed on the other samples, is detected in the “in situ” IR spectra (**Figure 5B**). This band, already observed in their reduced state prior to FT reaction, increases in intensity under FT conditions and has been ascribed to  $\text{Co}^{\delta+}$  sites in the cobalt-support interface [73]. While those interface sites are mayoritary in particles of small size, their increase under FT reaction conditions results from morphological changes in the small cobalt nanoparticle, as already detected by HRTEM, where a flattening of the cobalt particle is observed after FT reaction, enhancing the amount of metal interface sites. Since the electropositive character of the  $\text{Co}^{\delta+}$  sites inhibits CO dissociation, a higher amount of these sites turn out in a lower FT activity, explaining in that way the lower FT catalytic activity observed at small Co particle sizes. This result is interesting from a fundamental point of view explaining the nonclassical particle size-dependent FT activity and more importantly from a scientific point of view, highlighting the dynamism of catalysts under reaction condition and their impact on their catalytic performance, which has been underestimated in many studies. In this context, thanks to the recent development of advances of the spectroscopic tools with “in situ” capabilities, a lot of progress has been done in this direction, not only in the FT reaction but also in other catalytic processes, revealing a highly dynamic behavior of the catalysts at working conditions [74, 75].

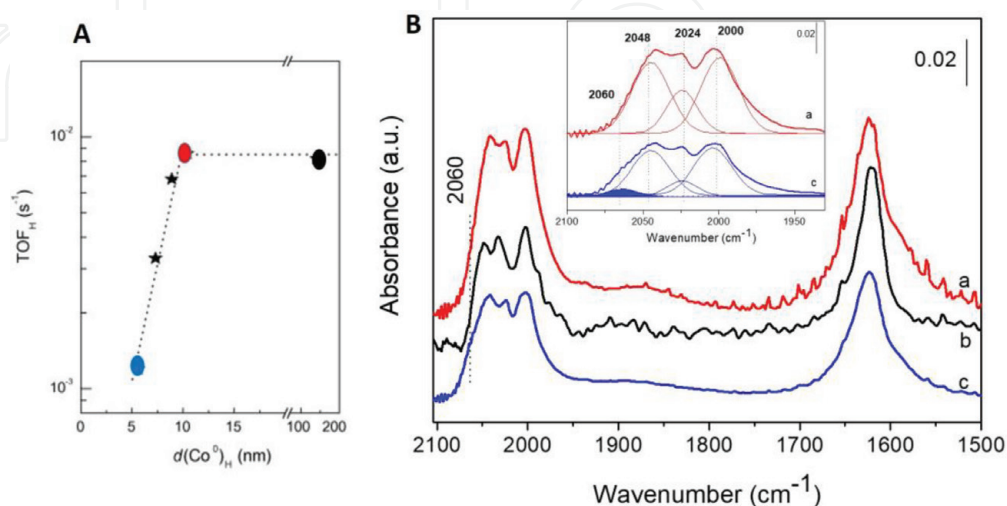


**Figure 5.** (A) Variation of the turnover frequency (TOF) in FT at 220°C and 20 bar with the cobalt particle size. (B) IR spectra after 4 h on stream in FT (220°C, 1 bar) for (a) Co-ITQ-2 with 10.4 nm Co particle size, (b) Co/SiO<sub>2</sub> with 141 nm Co particle size, and (c) Co-ITQ-2 with 5.6 nm Co particle size samples. In the inset the deconvolution of the Co-carbonyl region highlighting the presence of the 2060  $\text{cm}^{-1}$  IR band.



## 2.3 Determination of reaction mechanism and rate-limiting reaction step

Besides the characterization of catalyst surface sites, the identification of reaction intermediate species and reaction mechanism in a catalytic process is of great interest. It allows to define the rate-limiting reaction step, which coupled to a fundamental knowledge of the nature of active sites involved in each elementary step, enables a rational design of industrial catalysts. However, due to the transient nature of reaction intermediates, differentiating them from other species present in the catalyst but not being involved in the catalytic process (called as spectators) is often difficult. Ways to do it are following the evolution of surface species during time- and temperature-resolved IR experiments and combining the IR data with catalytic data obtained either “in situ” in coupled GC–MS analysis or in “ex situ” studies. The same can be done performing pressure-dependent IR studies. Next, an example will be presented that is supported by temperature-resolved IR studies, and different reaction mechanisms are established depending on the catalyst properties.

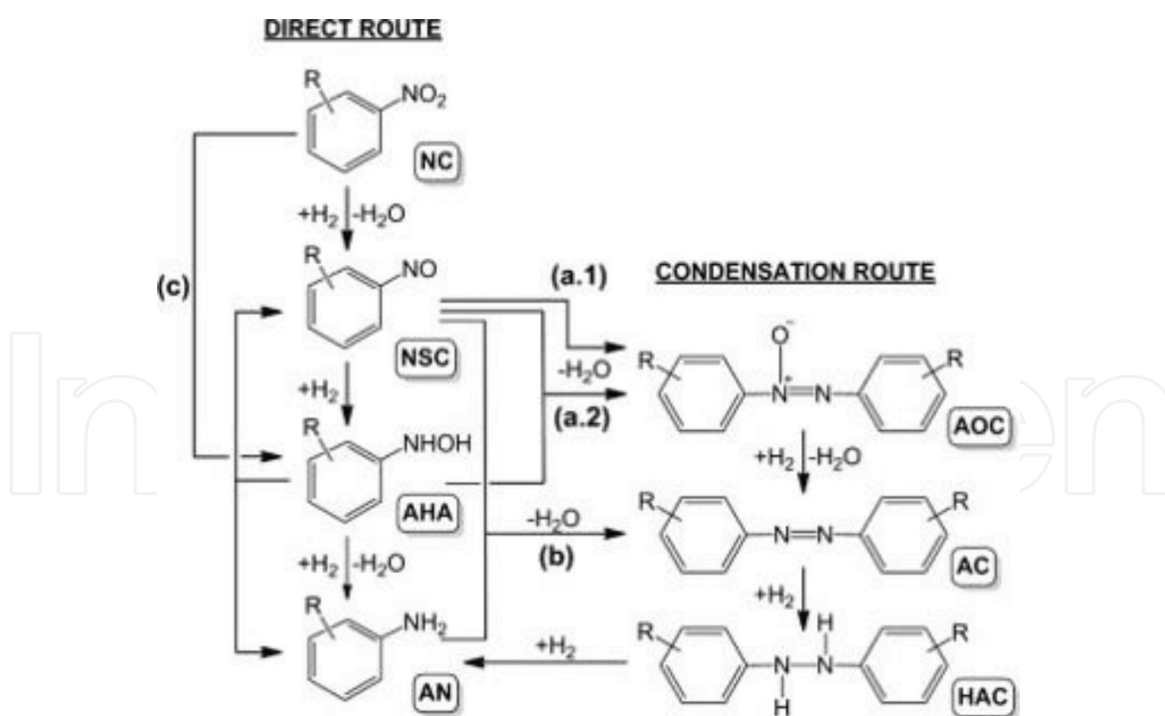
### 2.3.1 Hydrogenation of nitroaromatics on supported gold catalysts

Experiments performed in our laboratory have shown that under the same reaction conditions ( $T = 120^{\circ}\text{C}$ ,  $P = 4$  bar  $\text{H}_2$ ,  $[\text{Au}] = 1\%$ mol, Nitrobenzene = 0.25 M), Au nanoparticles of 2.5–3.5 nm particle size deposited on ceria ( $\text{Au}/\text{CeO}_2$ ) and on titania ( $\text{Au}/\text{TiO}_2$ ) display different selectivities in the hydrogenation of nitrobenzene. Thus, aniline is predominately formed on  $\text{Au}/\text{TiO}_2$  (~90% selectivity at 97% conversion), while azobenzene (~99% selectivity at 100% conversion) is formed on the  $\text{Au}/\text{CeO}_2$  catalyst [76]. Both aniline and azobenzene are valuable intermediates in the industrial production of pharmaceuticals, agrochemicals, pigments, dyes, and food additives, conferring high interest in the possibility to tune in a rational way the selectivity to the desired product by modifying the nature of the catalyst. If one considers the general reaction scheme proposed by Haber to reduce nitroaromatics (**Scheme 2**), it seems that the different catalytic performance of both  $\text{Au}/\text{TiO}_2$  and  $\text{Au}/\text{CeO}_2$  catalysts has to be related to a different reaction route (direct route versus condensation route), but the question is why both catalysts follow different reaction paths, and why in the case of the condensation route aniline is not formed as the final product. In order to answer this question, IR studies combined with micro-kinetic studies have been performed on both catalysts.

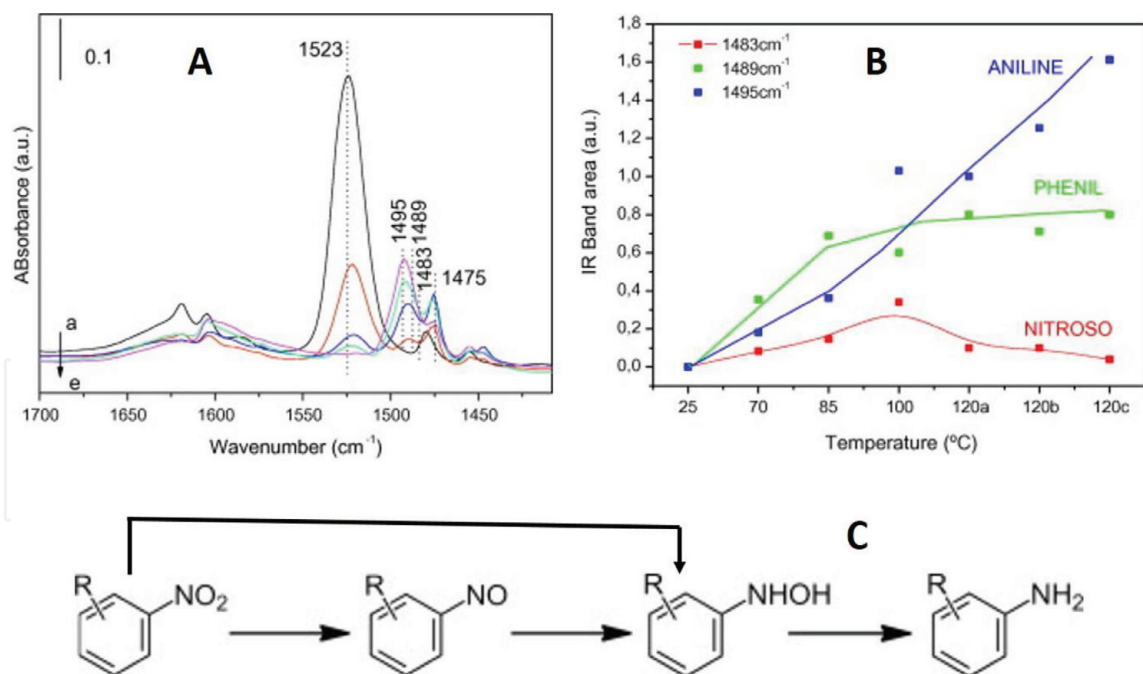
#### 2.3.1.1 IR studies of the hydrogenation of nitrobenzene on $\text{Au}/\text{TiO}_2$ catalysts

The hydrogenation of nitrobenzene is followed by IR on the  $\text{Au}/\text{TiO}_2$  catalysts performing temperature-dependent studies. In the IR spectra (**Figure 6A**), simultaneous to the consumption of nitrobenzene (IR bands at  $1523\text{ cm}^{-1}$ ), nitrosobenzene ( $1483, 1475\text{ cm}^{-1}$ ), phenylhydroxylamine ( $1489\text{ cm}^{-1}$ ), and aniline ( $1495\text{ cm}^{-1}$ ) are formed [77, 78]. The micro-kinetic data IR displayed in **Figure 6B** shows a low surface concentration of nitrosobenzene and a high amount of phenylhydroxylamine. Being phenylhydroxylamine an intermediate compound (see **Scheme 2**), its high surface concentration indicates a low hydrogenation rate to aniline and the coexistence of an additional parallel direct reaction path of phenylhydroxylamine formation starting from nitrobenzene in which nitrosobenzene formation is circumvented (**Figure 6C**). These results and the absence of IR bands of azoxy and/or azocompounds help to propose a direct hydrogenation route. Moreover, it is shown that the low surface concentration of nitrosobenzene during nitrobenzene hydrogenation is clue in this reaction path.



**Scheme 2.**

Reaction pathways in the hydrogenation of nitrocompounds to anilines. NC = nitrocompound, NSC = nitrosocompound, AHA = aromatic hydroxylamine, AN = aniline, AOC = azoxycompound, AC = azo compound, HAC = hydrazo compound [76].

**Figure 6.**

(A) IR spectra in the hydrogenation of nitrobenzene on Au/TiO<sub>2</sub> catalyst at (a) 25°C, (b) 70°C, (c) 85°C, (d) 100°C, and (e) 120°C (0.5 mbar NB and 8 mbar H<sub>2</sub>). (B) Evolution of the IR surface reaction intermediates species with temperature. (C) Proposed reaction path.

This is confirmed by additional IR experiments where the surface coverage of nitrosobenzene on the Au/TiO<sub>2</sub> catalyst is modified and the evolution of surface species under hydrogenation conditions monitored. Thus, at low surface coverage, a fast hydrogenation of nitrosobenzene to phenylhydroxylamine is observed,

followed by further hydrogenation to aniline, whereas at high nitrosobenzene coverage, azoxybenzene is mainly formed [76].

### 2.3.1.2 IR studies of the hydrogenation of nitrobenzene on Au/CeO<sub>2</sub> catalysts

In the temperature-dependent nitrobenzene hydrogenation IR studies performed on the Au/CeO<sub>2</sub> catalyst, nitrobenzene (IR bands at 1509 and 1343 cm<sup>-1</sup>) disappears slowly, followed by nitrosobenzene formation (1540, 1491, and 1398 cm<sup>-1</sup>) (**Figure 7A**). Nitrosobenzene is stabilized on the catalyst surface until 100°C, temperature at which azoxybenzene (IR bands at 1546, 1372, and 1357 cm<sup>-1</sup>) is formed. Increasing temperature to 120°C azobenzene (IR bands at 1303 and 1566 cm<sup>-1</sup>) is formed, showing a maximum at 21 min of reaction and then starting to decrease. This is associated to desorption of azobenzene to the gas phase, avoiding in that way a progressive hydrogenation to aniline and explaining the high selectivity to azobenzene displayed by the Au/CeO<sub>2</sub> catalyst [76]. These results are in line with a condensation route favored by an accumulation of nitrosobenzene on the catalyst surface. Moreover, previous IR results show a very fast reactivity of nitrosobenzene with phenylhydroxylamine, even at 25°C, giving azoxybenzene. Based on it, the surface accumulation of nitrosobenzene in the hydrogenation of nitrobenzene on the Au/CeO<sub>2</sub> catalyst, the absence of phenylhydroxylamine in the IR spectra, and the onset of azoxybenzene formation at 100°C indicate that the hydrogenation rate of nitrosobenzene to phenylhydroxylamine is low, being this the rate-limiting step. In conclusion, from these results, the different reaction pattern observed on the Au/CeO<sub>2</sub> catalysts is related to the stabilization of nitrosobenzene on the CeO<sub>2</sub> surface, which is ascribed to their basic properties compared to the TiO<sub>2</sub> as support.

Accordingly, these results show that it is possible to modulate the selectivity in the one-step nitroaromatic hydrogenation by adjusting the catalyst properties modulating in that way the concentration of nitrosobenzene on the catalyst surface.

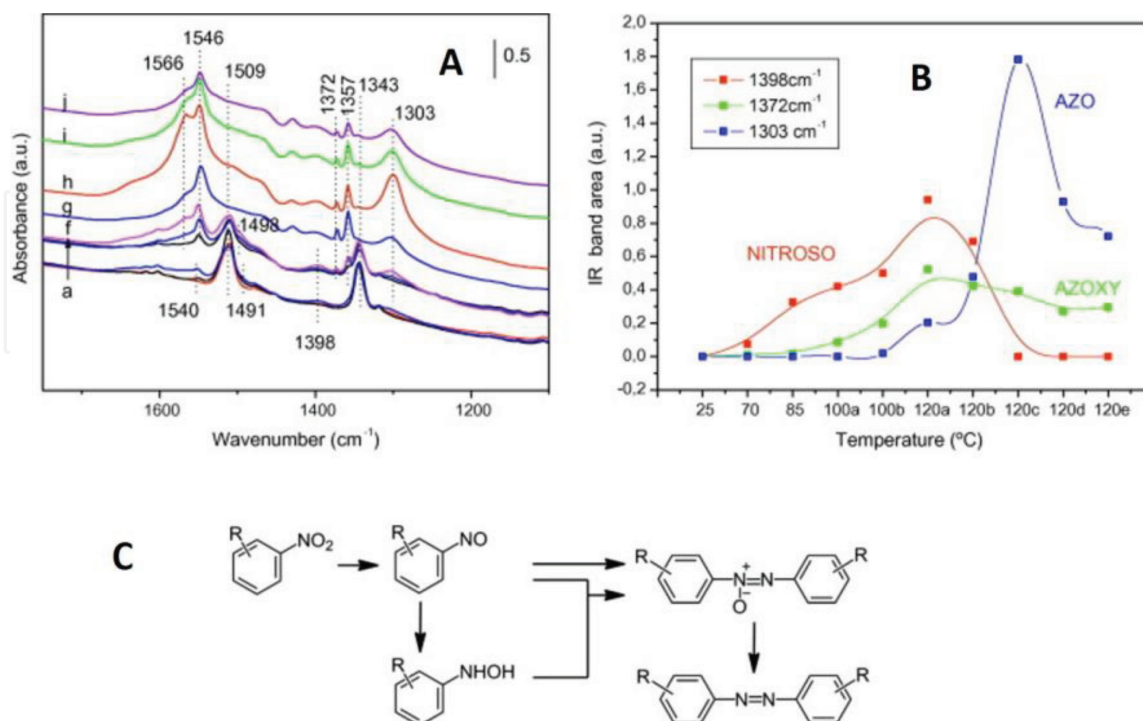


**Figure 7.** (A) IR spectra in the hydrogenation of nitrobenzene on Au/CeO<sub>2</sub> catalyst at (a) 25°C, (b) 70°C, (c) 85°C, (d) 100°C 10 min, (e) 100°C 30 min, (f) 120°C 7 min, (g) 120°C 17 min, (h) 120°C 21 min, (i) 120°C 26 min, and (j) 120°C 46 min (0.5 mbar NB and 8 mbar H<sub>2</sub>). (B) Evolution of the IR surface reaction intermediates species with temperature. (C) Proposed reaction path.

### 3. Conclusion

IR spectroscopy has been shown as a very powerful technique in the field of catalysis, enabling important information difficult to obtain with other techniques. Thus, surface sites and active species can be properly analyzed, which combined with the analysis of the reaction mechanism and the rate-limiting step are key points to direct the synthesis of catalysts with improved selectivity. Moreover, the dynamism of catalyst surfaces under reaction conditions monitored by IR spectroscopy has been highlighted, a fact usually underestimated but with strong repercussion on the catalytic performance.

### Acknowledgements

PC thanks the financial support of the Spanish government “Severo Ochoa Program” (SEV-2016-0683).

### Conflict of interest

There is no conflict of interest in this publication.


### Author details

Patricia Concepción

Instituto de Tecnología Química, Universitat Politècnica de València-Consejo Superior de Investigaciones Científicas (UPV-CSIC), Valencia, Spain

\*Address all correspondence to: [pconcepc@upvnet.upv.es](mailto:pconcepc@upvnet.upv.es)

### IntechOpen

© 2018 The Author(s). Licensee IntechOpen. This chapter is distributed under the terms of the Creative Commons Attribution License (<http://creativecommons.org/licenses/by/3.0>), which permits unrestricted use, distribution, and reproduction in any medium, provided the original work is properly cited. 

## References

- [1] Centi G, Perathoner S. Catalysis and sustainable (green) chemistry. *Catalysis Today*. 2003;**77**:287-297
- [2] Corma A, Serna P, Concepción P, Calvino JJ. Transforming nonselective into chemoselective metal catalysts for the hydrogenation of substituted nitroaromatics. *Journal of the American Chemical Society*. 2008;**130**:8748-8753. DOI: 10.1021/ja800959g
- [3] Boronat M, Concepción P. Combined theoretical and spectroscopic mechanistic studies for improving activity and selectivity in heterogeneous catalysis. *Catalysis Today*. 2017;**285**: 166-178. DOI: 10.1016/j.cattod.2016.11.048
- [4] Zaera F. New advances in the use of infrared adsorption spectroscopy for the characterization of heterogeneous catalytic reactions. *Chemical Society Reviews*. 2014;**43**:7624-7663. DOI: 10.1039/c3cs60374a
- [5] Bordiga S, Lamberti C, Bonino F, Travert A, Thibault-Starzyk F. Probing zeolites by vibrational spectroscopies. *Chemical Society Reviews*. 2015;**44**: 7262-7341. DOI: 10.1039/c5cs00396b
- [6] Ryczkowski J. IR spectroscopy in catalysis. *Catalysis Today*. 2001;**68**: 263-381. DOI: 10.1016/S0920-5861(01)00334-0
- [7] Peri JB. Infrared spectroscopy in catalytic Research. In: Anderson JR, Boudart M, editors. *Catalysis. Catalysis (Science and Technology)*. Vol. 5. Berlin, Heidelberg: Springer; 1984. pp. 171-220. DOI: 10.1007/978-3-642-93247-2\_3
- [8] Vimont A, Thibault-Starzyk F, Daturi M. Analysing and understanding the active sites by IR spectroscopy. *Chemical Society Reviews*. 2010;**39**: 4928-4950. DOI: 10.1039/B919543M
- [9] Meunier FC. The design and testing of kinetically- appropriate operando spectroscopic cells for investigating heterogeneous catalytic reactions. *Chemical Society Reviews*. 2010;**39**: 4602-4614. DOI: 10.1039/B919705M
- [10] Foster AJ, Lobo RF. Identifying reaction intermediates and catalytic active sites through in situ characterization techniques. *Chemical Society Reviews*. 2010;**39**:4783-4793. DOI: 10.1039/C0CS00016G
- [11] Eli S, Weckhuysen BM. Infrared and Raman image of heterogeneous catalysts. *Chemical Society Reviews*. 2010;**39**:4615-4625. DOI: 10.1039/C0CS00064G
- [12] Bentrup U. Combining in situ characterization methods in one set-up: Looking with more eyes into the intricate chemistry of the synthesis and working of heterogeneous catalysts. *Chemical Society Reviews*. 2010;**39**: 4718-4730. DOI: 10.1039/B919711G
- [13] Newton MA, Von Beek W. Combining synchrotron-based X-ray techniques with vibrational spectroscopies for the in situ study of heterogeneous catalysts: A view from a bridge. *Chemical Society Reviews*. 2010;**39**:4845-4863. DOI: 10.1039/B919689G
- [14] Gribov EN, Cocina D, Spoto G, Bordiga S, Ricchiardi G, Zecchina A. Vibrational and thermodynamic properties of Ar, N<sub>2</sub>, O<sub>2</sub>, H<sub>2</sub> and CO adsorbed and condensed into (H,N<sub>a</sub>)-Y zeolite cages as studied by variable temperature IR spectroscopy. *Physical Chemistry Chemical Physics*. 2006;**8**: 1186-1196. DOI: 10.1039/B513367J
- [15] Arean CO, Delgado MR, Bibiloni GF, Bludský O, Nachtigall P. Variable-temperature IR spectroscopic and theoretical studies on CO<sub>2</sub> adsorbed in



- zeolite K-FER. *Chemphyschem.* 2011;**12**: 1435-1443. DOI: 10.1002/cphc.201000995
- [16] Knözinger H, Huber S. IR spectroscopy of small and weakly interacting molecular probes for acidic and basic zeolites. *Journal of the Chemical Society, Faraday Transactions.* 1998;**94**:2047-2059. DOI: 10.1039/A802189I
- [17] Lavalley JC. Infrared spectrometric studies of the surface basicity of metal oxides and zeolites using adsorbed probe molecules. *Catalysis Today.* 1996;**27**:377-401. DOI: 10.1016/0920-5861(95)00161-1
- [18] Davydov A. *Molecular Spectroscopy of Oxide Catalyst Surfaces.* Hoboken, NJ: John Wiley&Sons, Inc.; 2003. ISBN 0-417-98731-X
- [19] Busca G. Spectroscopic characterization of the acid properties of metal oxide catalysts. *Catalysis Today.* 1998;**41**:191-206. DOI: 10.1016/S0920-5861(98)00049-2
- [20] Lercher JA, Gründling C, Eder-Mirth G. Infrared studies of the surface acidity of oxides and zeolites using adsorbed probe molecular. *Catalysis Today.* 1996;**27**:353-376. DOI: 10.1016/0920-5861(95)00248-0
- [21] Zecchina A, Scarano D, Bordiga A, Ricchiardi G, Spoto G, Geobaldo F. IR studies of CO and NO adsorbed on well characterized oxide single microcrystals. *Catalysis Today.* 1996;**27**(3-4):403-435. DOI: 10.1016/0920-5861(95)00202-2
- [22] Bordiga S, Regli L, Cocina D, Lamberti C, Bjørgen M, Lillerud KP. Assessing the acidity of high silica chabazite H-SSZ-13 by FTIR using CO as molecular probe: Comparison with H-SAPO-34. *The Journal of Physical Chemistry. B.* 2005;**109**:2779-2784. DOI: 10.1021/jp045498w
- [23] Daniell W, Topsoe NY, Knözinger H. An FTIR study of the surface acidity of USY zeolites: Comparison of CO, CD<sub>3</sub>CN and C<sub>5</sub>H<sub>5</sub>N probe molecules. *Langmuir.* 2001;**17**(20):6233-6239. DOI: 10.1021/la010345a
- [24] Kondo JN, Nishitani R, Yoda E, Yokoi T, Tatsumi T, Domen K. A comparative IR characterization of acid sites on HY zeolite by pyridine and CO probes with silica-alumina and  $\gamma$ -alumina references. *Physical Chemistry Chemical Physics.* 2010;**12**:11576-11586. DOI: 10.1039/C0CP00203H
- [25] Morterra C, Mentrui MP, Cerrato G. Acetonitrile adsorption as an IR spectroscopic probe for surface acidity/basicity of pure and modified zirconias. *Physical Chemistry Chemical Physics.* 2002;**4**:676-687. DOI: 10.1039/B109047J
- [26] Giordanino F, Vennestrom PN, Lundegaard LF, Stappen FN, Mossin S, Beato P, Bordiga S, Lamberti C. Characterization of Cu-exchanged SSZ-13: A comparative FTIR, UV-VIS, and EPR study with Cu-ZSM-5 and Cu- $\beta$  with similar Si/Al and Cu/Al ratios. *Dalton Transactions.* 2012;**42**(35): 1274-12761. DOI: 10.1039/c3dt50732g
- [27] Wang D, Zhang L, Kamasamudram K, Epling WS. In situ -DRIFT study of selective catalytic reduction of NO<sub>x</sub> by NH<sub>3</sub> over Cu-exchanged SAPO-34. *ACS Catalysis.* 2013;**3**:871-881. DOI: 10.1021/cs300843k
- [28] Borfecchia E, Lomachenko KA, Giordanino F, Falsig H, Beato P, Soldatov AV, Bordiga S, Lamberti C. Revisiting the nature of Cu sites in the activated Cu-SSZ-13 catalyst for SCR reaction. *Chemical Science.* 2015;**6**: 548-563. DOI: 10.1039/c4sc02907k
- [29] Martínez-Franco R, Moliner M, Franch C, Kustov A, Corma A. Rational direct synthesis methodology of very active and hydrothermally stable Cu-SAPO-34 molecular sieves for the SCR

of NO<sub>x</sub>. Applied Catalysis B: Environmental. 2012;**127**:273-280. DOI: 10.1016/j.apcatb.2012.08.034

Catalysis. Journal of Physical Chemistry C. 2009;**113**:16772-16784. DOI: 10.1021/jp905157r

[30] Martínez-Franco R, Moliner M, Concepcion P, Thogersen JR, Corma A. Synthesis, characterization and reactivity of highly hydrothermally stable Cu-SAPO-34 materials prepared by "one pot" processes. Journal of Catalysis. 2014;**314**:73-82. DOI: 10.1016/j.jcat.2014.03.018

[36] Bosch E, Huber S, Weitkamp J, Knözinger H. Adsorption of trichloro- and trifluoromethane in Y-zeolites as studied by IR spectroscopy and multinuclear solid-state NMR. Physical Chemistry Chemical Physics. 1999;**1**: 579-584. DOI: 10.1039/A808296K

[31] Martínez-Franco R, Moliner M, Thogersen JR, Corma A. Efficient one-pot preparation of Cu-SSZ-13 materials using cooperative OSDAs for their catalytic application in the SCR of NO<sub>x</sub>. ChemCatChem. 2013;**5**:3316-3323. DOI: 10.1002/cctc.201300141

[37] Köck EM, Kogler M, Bielz T, Klötzer B, Penner S. In situ FT-IR spectroscopic study of CO<sub>2</sub> and CO adsorption on Y<sub>2</sub>O<sub>3</sub>, ZrO<sub>2</sub>, and Yttria-stabilized ZrO<sub>2</sub>. The Journal of Physical Chemistry. C, Nanomaterials and Interfaces. 2013;**117**: 17666-17673. DOI: 10.1021/jp405625x

[32] Concepción P, Boronat M, Millán R, Moliner M, Corma A. Identification of distinct copper species in Cu-CHA samples using NO as probe molecule. A combined IR spectroscopic and DFT study. Topics in Catalysis. 2017;**60**: 1653-1663. DOI: 10.1007/s11244-017-0844-7

[38] Menéndez-Rodríguez L, Tomás-Mendivil E, Francos J, Nájera C, Crochet P, Cadierno V. Palladium (II) complexes with a phosphino-oxime ligand: Synthesis, structure and applications to the catalytic rearrangement and dehydration of aldoximes. Catalysis Science & Technology. 2015;**5**: 3754-3761. DOI: 10.1039/C5CY00413F

[33] Concepción P, Corma A, Silvestre-Albero J, Franco V, Chane-Ching JY. Chemoselective hydrogenation catalysts: Pt on mesostructure CeO<sub>2</sub> nanoparticles embedded within ultrathin layers of SiO<sub>2</sub> binder. Journal of the American Chemical Society. 2004;**126**:5523-5532. DOI: 10.1021/ja031768x

[39] Tamilselvan P, Basavaraju YB, Sampathkumar E, Murugesan R. Cobalt (II)catalyzed dehydration of aldoximes: A highly efficient practical procedure for the synthesis of nitriles. Catalysis Communications. 2009;**10**(5):716-719. DOI: 10.1016/j.catcom.2008.11.025

[34] Yudanov IV, Sahnoun R, Neyman KM, Rösch N, Hoffmann J, Schauermaun S, et al. CO adsorption on Pd nanoparticles: Density functional and vibrational spectroscopy studies. Journal of Physical Chemistry. 2003;**107**:255-264. DOI: 10.1021/jp022052b

[40] Yan P, Batamack P, Prakash GKS, Olah GA. Gallium (III) triflate catalyzed dehydration of aldoximes. Catalysis Letters. 2005;**101**:141-143. DOI: 10.1007/s10562-005-4880-8

[35] Boronat M, Concepción P, Corma A. Unravelling the nature of gold surface sites by combining IR spectroscopy and DFT calculations. Implications in

[41] Behbahani FK, Heravi MM, Oskooie HA. Highly efficient dehydration of aldoximes in the presence of Fe(ClO<sub>4</sub>)<sub>3</sub> as catalyst. In: Taylor JC, editor. Advances in Chemistry Research. Vol. 7. 1st quartier. New York: Nova Science Publishers, Hauppauge; 2011. pp. 253-257. ISBN: 978-1-61761-898-7

- [42] Rapeyko A, Climent MJ, Corma A, Concepción P, Iborra S. Postsynthesis-treated iron-based metal-organic frameworks as selective catalysts for the sustainable synthesis of nitriles. *ChemSusChem*. 2015;8:3270-3282. DOI: 10.1002/cssc.201500695
- [43] Choi E, Lee C, Na Y, Chang S.  $[\text{RuCl}_2(\text{p-cymene})]_2$  on carbon: An efficient, selective, reusable, and environmentally versatile heterogeneous catalyst. *Organic Letters*. 2002;4(14):2369-2371. DOI: 10.1021/ol0260977
- [44] Rapeyko A, Climent MJ, Corma A, Concepción P, Iborra S. Nanocrystalline  $\text{CeO}_2$  as a highly active and selective catalyst for the dehydration of aldoximes to nitriles and one-pot synthesis of amides and esters. *ACS Catalysis*. 2016;6:4564-4575. DOI: 10.1021/acscatal.6b00272
- [45] Sirijaraensre J, Limtrakul J. Structures and mechanism of the dehydration of benzaldoxime over Fe-ZSM-5 zeolites: A DFT study. *Structural Chemistry*. 2013;24(4):1307-1318. DOI: 10.1007/s11224-012-0161-5
- [46] Mc Guinness D. Olefin oligomerization via metallacycles: Dimerization, trimerization, tetramerization, and beyond. *Chemical Reviews*. 2011;111(3):2321-2341. DOI: 10.1021/cr100217q
- [47] Lallemand M, Finiels A, Fajula F, Hulea V. Catalytic oligomerization of ethylene over Ni-containing dealuminated Y zeolites. *Applied Catalysis A: General*. 2006;301:196-201. DOI: 10.1016/j.apcata.2005.12.019
- [48] Martínez A, Arribas MA, Concepción P, Moussa S. New bifunctional Ni-H-beta catalysts for the heterogeneous oligomerization of ethylene. *Applied Catalysis A: General*. 2013;467:509-518. DOI: 10.1016/j.apcata.2013.08.021
- [49] Agirrezabal-Telleria I, Iglesia E. Stabilization of active, selective, and regenerable Ni-based dimerization catalysts by condensation of ethene within ordered mesoporous. *Journal of Catalysis*. 2017;352:505-514. DOI: 10.1016/j.jcat.2017.06.025
- [50] Tanaka M, Itadani A, Kuroda Y, Iwamoto M. Effect of pore size and nickel content of Ni-MCM-41 on catalytic activity for Ethene dimerization and local structures of nickel ions. *Journal of Physical Chemistry C*. 2012;116:5664-5672. DOI: 10.1021/jp2103066
- [51] Moussa S, Arribas MA, Concepción P, Martínez A. Heterogeneous oligomerization of ethylene to liquids on bifunctional Ni-based catalysts: The influence of support properties on nickel speciation and catalytic performance. *Catalysis Today*. 2016;277:78-88. DOI: 10.1016/j.cattod.2015.11.032
- [52] Andrei RD, Popa MI, Fajula F, Hulea V. Heterogeneous oligomerization of ethylene over highly active and stable Ni- $\text{AlSBA-15}$  mesoporous catalysts. *Journal of Catalysis*. 2015;323:76-84. DOI: 10.1016/j.jcat.2014.12.027
- [53] Moussa S, Concepción P, Arribas MA, Martínez A. Nature of active sites and initiation mechanism for ethylene oligomerization on heterogeneous Ni-beta catalysts. *ACS Catalysis*. 2018;8:3903-3912. DOI: 10.1021/acscatal.7b03970
- [54] Mihaylov M, Hadjiivanov K. FTIR study of CO and NO adsorption and coadsorption on Ni-ZSM-5 and Ni/ $\text{SiO}_2$ . *Langmuir*. 2002;18:4376-4383. DOI: 10.1021/la015739g
- [55] Hadjiivanov K, Mihaylov M, Klissurski D, Stefanov P, Abadjieva N, Vassileva E, Mintchev L. Characterization of Ni/ $\text{SiO}_2$  catalysts prepared by successive deposition and reduction of  $\text{Ni}^{2+}$  ions. *Journal of*



Catalysis. 1999;**185**:314-323. DOI: 10.1006/jcat.1999.2521

[56] Penkova A, Dzwigaj S, Kefirov R, Hadjiivanov K, Che M. Effect of the preparation method on the state of nickel ions in BEA zeolites. A study by Fourier transform infrared spectroscopy of adsorbed CO and NO, temperature reduction, and X-ray diffraction. *Journal of Physical Chemistry C*. 2007; **111**(24):8623-8631. DOI: 10.1021/jp071927p

[57] Dry ME. The Fischer-Tropsch process-commercial aspects. *Catalysis Today*. 1990;**6**(3):183-206. DOI: 10.1016/0920-5861(90)85002-6

[58] Iglesia E. Design, synthesis, and use of cobalt-based Fischer-Tropsch synthesis catalysts. *Applied Catalysis A: General*. 1997;**161**:59-78. DOI: 10.1016/S0926-860X(97)00186-5

[59] Reuel RC, Bartholomew CH. Effects of support and dispersion on the CO hydrogenation activity/selectivity properties of cobalt. *Journal of Catalysis*. 1984;**85**:78-88. DOI: 10.1016/0021-9517(84)90111-8

[60] Martínez A, López C, Márquez F, Díaz I. Fischer-Tropsch synthesis of hydrocarbons over mesoporous Co/SBA-15 catalysts: The influence of metal loading, cobalt precursor, and promoters. *Journal of Catalysis*. 2003; **220**(2):486-499. DOI: 10.1016/S0021-9517(03)00289-6

[61] Khodakov AY, Griboval-Constant A, Bechara R, Zholobenko VL. Pore size effects in Fischer-Tropsch synthesis over cobalt-supported mesoporous Silicas. *Journal of Catalysis*. 2002; **206**(2):230-241. DOI: 10.1006/jcat.2001.3496

[62] Kim DJ, Dunn BC, Cole P, Turpin G, Ernst RD, Pugmire RJ, Kang M, Kim JM, Eyring EM. Enhancement in the reducibility of cobalt oxides on a

mesoporous silica supported cobalt catalyst. *Chemical Communications*. 2005:1462-1464. DOI: 10.1039/b417536k

[63] Bezemer GL, Bitter JH, Kuipers HP, Oosterbeek H, Holeyijn JE, Kapteijn F, Van Dillen AJ, De Jong KP. Cobalt particle size effects in the Fischer-Tropsch reaction studied with carbon nanofiber supported catalysts. *Journal of the American Chemical Society*. 2006; **128**(12):3956-3964. DOI: 10.1021/ja058282w

[64] Barbier A, Tuel A, Arcon I, Kodre A, Martin GA. Characterization and catalytic behaviour of Co/SiO<sub>2</sub> catalysts: Influence of dispersion in the Fischer-Tropsch reaction. *Journal of Catalysis*. 2001;**200**(1):106-116. DOI: 10.1006/jcat.2001.3204

[65] Prieto G, Martínez A, Concepción P, Moreno-Tost R. Cobalt particle size effects in Fischer-Tropsch synthesis: Structural and in situ spectroscopic characterisation on reverse micelle-synthesised Co/ITQ-2 model catalysts. *Journal of Catalysis*. 2009;**266**:129-144. DOI: 10.1016/j.jcat.2009.06.001

[66] Song D, Li J, Cai Q. In situ diffuse reflectance FTIR study of CO adsorbed on a cobalt catalyst supported by Silia with different pore sizes. *Journal of Physical Chemistry C*. 2007;**11**: 18970-18979. DOI: 10.1021/jp0751357

[67] Hu Z, Mo L, Feng X, Shi J, Wang Y, Xie Y. Synthesis and electrochemical capacitance of sheet-like cobalt hydroxide. *Materials Chemistry and Physics*. 2009;**114**:53-57. DOI: 10.1016/j.matchemphys.2008.07.073

[68] Prieto G, Concepción P, Murciano R, Martínez A. The impact of pre-reduction thermal history on the metal surface topology and site-catalytic activity of Co/SiO<sub>2</sub> Fischer-Tropsch catalysts. *Journal of Catalysis*. 2013;**302**: 37-48. DOI: 10.1016/j.jcat.2013.02.022



- [69] Rygh LES, Nielsen CJ. Infrared study of CO adsorbed on a Co/Re/ $\gamma$ -Al<sub>2</sub>O<sub>3</sub>-based Fischer-Tropsch catalyst. *Journal of Catalysis*. 2000;**194**(2): 401-409. DOI: 10.1006/jcat.2000.2955
- [70] Anson CE, Powell DB. The metal-carbide stretching frequencies in the clusters [M<sub>5</sub>C(CO)<sub>15</sub>] (M=Ru, Os) and their derivatives as an aid to cluster structure determination. *Journal of Molecular Structure*. 1987;**159**:11-17. DOI: 0022-2860/87
- [71] Lavrentiev V, Abe H, Yamamoto S, Naramoto H, Narumi K. Formation of promising Co-C nanocompositions. *Surface and Interface Analysis*. 2003;**35**: 36-39. DOI: 10.1002/sia.1489
- [72] Ciobica IM, Van Santen RA, Van Berge PJ, Van de Loosdrecht J. Adsorbate induced reconstruction of cobalt surfaces. *Surface Science*. 2008; **602**(1):17-27. DOI: 10.1016/j.susc.2007.09.060
- [73] Rygh LES, Ellestad OH, Klæboe P, Nielsen CJ. Infrared study of CO adsorbed on Co/ $\gamma$ -Al<sub>2</sub>O<sub>3</sub> based Fischer-Tropsch catalysts; semi-empirical calculations as a tool for vibrational assignments. *Physical Chemistry Chemical Physics*. 2000;**2**:1835-1846. DOI: 10.1039/B000188K
- [74] Moliner M, Gabay JE, Kliewer CE, Carr RT, Guzman J, Casty GL, Serna P, Corma A. Reversible transformation of Pt nanoparticles into single atoms inside high-silica chabazite zeolite. *Journal of the American Chemical Society*. 2016; **138**(48):15743-15750. DOI: 10.1021/jacs.6b10169
- [75] Liu L, Zakharov DN, Arenal R, Concepción P, Stach EA, Corma A. Evolution and stabilization of subnanometric metal species in confined space by in situ TEM. *Nature Communications*. 2018;**9**:574-584. DOI: 10.1038/s41467-018-03012-6
- [76] Combata D, Concepción P, Corma A. Gold catalysts for the synthesis of aromatic azocompounds from nitroaromatics in one step. *Journal of Catalysis*. 2014;**311**:339-349. DOI: 10.1016/j.jcat.2013.12.014
- [77] Boronat M, Concepción P, Corma A, González S, Illas F, Serna P. A molecular mechanism for the chemoselective hydrogenation of substituted nitroaromatics with nanoparticles of gold on TiO<sub>2</sub> catalysts: A cooperative effect between gold and the support. *Journal of the American Chemical Society*. 2007;**129**(51):16230-16237. DOI: 10.1021/ja076721g
- [78] Richner G, Van Bokhoven JA, Neuhold YM, Makosch M, Hungerbühler K. In situ infrared monitoring of the solid/liquid catalyst interface during the three-phase hydrogenation of nitrobenzene over nanosized Au on TiO<sub>2</sub>. *Physical Chemistry Chemical Physics*. 2011;**13**: 12463-12471. DOI: 10.1039/C1CP20238C